Basal Ventricular Septal Hypertrophy in Systemic Hypertension

Lončaric, Filip; Nunno, Loredana; Mimbrero, Maria; Marciniak, Maciej; Fernandes, Joao Filipe; Tirapu, Laia; Fabijanović, Dora; Sanchis, Laura; Doltra, Adelina; Čikeš, Maja; ...

Full title: Ventricular Basal Septal Hypertrophy in Systemic Hypertension

Running title: Basal Septal Hypertrophy in Hypertension

Author list:

Filip Loncaric[a] MD**,** Loredana Nunno[a,b] MD, Maria Mimbrero[a,b] MD, Maciej Marciniak[c] MSc, Joao Filipe Fernandes[c] MSc, Laia Tirapu[a,b] MD, Dora Fabijanovic[d] MD, Laura Sanchis[a,b] MD, PhD, Adelina Doltra[a,b] MD, PhD, Maja Cikes[d] MD, PhD, Pablo Lamata[c] PhD, Bart Bijnens[a,e*] PhD, Marta Sitges[a,b,f*] MD, PhD

Affiliations:

a. Institut d'Investigacions Biomèdiques August Pi i Sunyer (IDIBAPS), Barcelona, Spain
b. Cardiovascular Institute, Hospital Clínic and Universitat de Barcelona, Barcelona, Spain
c. Kings College London, Department of Biomedical Engineering, London, United Kingdom
d. University Hospital Centre Zagreb, Department for Cardiovascular Diseases and University of Zagreb School of Medicine, Zagreb, Croatia
e. La *Institució Catalana de Recerca i Estudis Avançats*, (ICREA), Barcelona, Spain
f. CIBERCV, Instituto de Salud Carlos III (CB16/11/00354); CERCA Programme / Generalitat de Catalunya

* Contributed equally as senior authors

Corresponding author:

Filip Loncaric, MD**;** IDIBAPS-Institut d'Investigacions Biomèdiques August Pi i Sunyer
Carrer del Rosselló, 149, 08036 Barcelona
Phone: +385912220480**,** E-mail: loncaric.filip@gmail.com

This is the pre-print, pre-peer reviewed version of the following article:

Loncaric F, Nunno L, Mimbrero M, Marciniak M, Fernandes JF, Tirapu L, et al. Basal Ventricular Septal Hypertrophy in Systemic Hypertension. Am J Cardiol. 2020 May 1;125(9):1339–46. 10. 10. https://doi.org/10.1016/j.amjcard.2020.01.045

Abstract

Basal septal hypertrophy (BSH) is commonly seen in patients with systemic hypertension and has been associated with increased afterload. The impact of localized hypertrophy on left ventricular (LV) and left atrial (LA) function is still unclear. Our aim is to investigate if BSH is a marker of a more pronounced impact of hypertension on cardiac function in the early stages of hypertensive heart disease. An echocardiogram was performed in 163 well-controlled hypertensive patients and 22 healthy individuals. BSH was defined by a basal-to-mid septal thickness ratio ≥ 1.4. LV dimensions and mass were evaluated. LV global and regional deformation was assessed by 2-dimensional (2D) speckle tracking echocardiography (STE), and LV diastolic function by 2D and Doppler imaging. LA function was evaluated with phasic volume indices calculated from 2D and 3-dimensional (3D) volumes, as well as STE. The population was 54% men, mean age 57 (53-60) years. BSH was seen in 20% (n=32) of the hypertensive cohort. Patients with BSH showed decreased regional LV systolic deformation, impaired LV relaxation with a higher proportion of indeterminate LV diastolic function, and LA functional impairment defined by a reduction of reservoir strain and a change in LA functional dynamics. In conclusion, in well-controlled hypertension impairment of LV and LA function is present in patients with early LV remodeling and localized hypertrophy. BSH might be useful as an early marker of the burden of hypertensive heart disease.

Keywords: hypertension, hypertrophy/remodeling, basal septal hypertrophy, speckle tracking echocardiography

Introduction

Concentric LV hypertrophy is the long-term physiological adaptation to a continued increase in afterload[1]. However, in early stages of hypertensive heart disease the increase in wall thickness is gradual, changes in wall thickness are not uniform[2] and a part of patients develop localized basal septal hypertrophy (BSH)[3–7]. The finding of BSH in volunteers with no prior history of elevated blood pressure has been shown to be related to masked hypertension.[1] While BSH can be seen in 2% of the general population, rising up to 18% in the elderly,[5] only a few studies have investigated the prevalence in hypertensive cohorts, finding it to be around 20%[3,8]. We hypothesize that hypertensive patients with BSH have a more extensive burden of the hypertensive disease with more impact on cardiac function. The aim of this research was therefore, to perform a comprehensive LV and LA assessment in well-controlled hypertensive patients, comparing cardiac function among those with and without BSH.

Methods

The cohort consisted of 163 hypertensive patients and 22 healthy individuals used as a control reference group. The participants were studied at two centers - Hospital Clinic Barcelona and the University Hospital Centre in Zagreb. Hypertensive patients with well-controlled blood pressure (BP < 130/80 mmHg by self-reported control), treated during a minimum of 3 years with antihypertensive drugs, were included. Patients were recruited from the out-patient clinic and from general practitioner referrals. Exclusion criteria were history of heart failure or previously known target organ disease. Healthy controls included volunteers from the local community, that were presumed healthy, without prior history of hypertension, diabetes or other significant cardiac or non-cardiac diseases. All participants underwent a clinical interview with survey about cardiovascular risk factors, family medical history, comorbidities, and pharmacological treatment

- followed by a comprehensive echocardiographic examination. The study was approved by the corresponding hospital ethical committees, and participants gave written informed consent.

Examinations were performed according to current recommendations[9] on a commercially available Vivid E9 or E95 system (GE, Vingmed Ultrasound, Horten, Norway) equipped with a M5S and 4Vc transthoracic transducer, respectively. Images were analyzed using Echopac software (GE Medical Systems, version 202.41.0). Participants were studied with 2D and Doppler echocardiography, as well as 2D speckle tracking deformation imaging. Real-time 3D scans of the LA were obtained with the probe in the apical position during breath-hold in hypertensive patients.

The anteroseptal and inferoseptal wall thickness were measured at end-diastole at basal- and mid-level in the parasternal long axis (PLAX) and 4-chamber cardiac views, respectively (**Figure 1**). Measurements were obtained in 2D images, with one caliper positioned on the interface between the myocardial wall and cavity and the other at the transition of the LV to the RV septal myocardium. BSH was defined based on the basal-to-mid septal wall thickness ratio of ≥ 1.4 in either the 4-chamber or PLAX view. LV mass was calculated by the linear method and normalized by body surface area, and sex-dependent cut-off values were used to indicate LV hypertrophy[9]. Relative wall thickness (RWT) was calculated by dividing the doubled value of the end-diastolic posterior wall thickness with the end-diastolic internal diameter of the LV. The type of LV remodeling was determined based on the RWT and indexed LV mass [9].

Deformation of the LV and LA was assessed using speckle tracking echocardiography (STE) software on 2D grayscale images obtained from the apical 4-chamber view. The analysis of LA deformation was performed in the 4- and 2-chamber apical views. Using the beginning of the P wave as the onset for deformation analysis, left atrial reservoir, conduit, and contractile function were evaluated by measuring LA systolic, early diastolic and late diastolic strain,

respectively and averaged from the 4- and 2-chamber measurements. LA function was additionally assessed using 2D and 3D LA volumes - the minimal, maximal, and the volume before atrial contraction at the beginning of the P wave. Standard indexes of LA function were calculated using volumes indexed to BSA - total ejection fraction, active and passive emptying fraction and the active contribution to LV filling.

Further details on echocardiography, LV mass calculation and the assessment of intra-observer and inter-observer reproducibility of septal thickness, ventricular and atrial strain measurements are described in the **Supplementary Materials**.

The data was analyzed using IBM SPSS Statistics version 23.0. The quantitative variables were expressed as mean ± standard deviation or median and interquartile range based on the normality of their distribution evaluated by the Shapiro-Wilk test. The qualitative variables as a total number and percentage. Differences between groups were analyzed for statistical significance with the ANOVA test when comparing variables with normal distribution and the Wilcoxon test for non-normally distributed variables. Post-hoc comparisons were assessed with the Bonferroni correction. When comparing categorical data, contingency tables and a Chi-square test were used. In the case the table contained a cell with the expected value of less than 5, the Fisher's exact test was used for comparison. A value of $p < 0.05$ was considered statistically significant.

Results

Clinical characteristics of the cohort are presented in **Table 1**. In the BSH subgroup, 88% (n=28) of the patients were classified as BSH in both 4C and PLAX views, whereas 9% (n=3) and 3% (n=1) had positive criteria for BSH only in the 4C and PLAX view, respectively.

Hypertensive patients and healthy controls had comparable age and gender characteristics (median age 57 vs. 54 years, male sex 55% vs. 46%). Hypertensive patients with BSH were older, with no differences considering the duration of hypertension, comorbidities - such as diabetes or dyslipidemia, or antihypertensive therapy as compared to those without BSH.

Characteristics of LV size and function are presented in **Table 2** and **Figure 2**. While all patients with BSH had abnormal LV geometry, it was normal in 17% of hypertensives without BSH and a majority of controls. LV ejection fraction and GLS was preserved in all groups; however, marked segmental abnormalities in LV systolic deformation were seen in hypertensive patients with BSH with a significant decline in longitudinal strain in the basal and mid-inferoseptum (**Figure 2)**.

There was a trend of lower mitral E and diastolic pulmonary vein velocities in the BSH patients as compared to hypertensive patients without BSH and the controls, while the mitral A velocity was higher - resulting in a significantly lower E/A ratio of the BSH subgroup. BSH was also associated with increased a' and lower e' velocities of the mitral annulus. IVRT showed a clear trend of prolongation in the hypertensive subgroups. Using the current algorithms for diagnosing diastolic dysfunction in patients with preserved ejection fraction, none of the participants fulfilled criteria for diastolic dysfunction. All healthy controls were diagnosed with normal diastolic function, whereas 8% (n=11) of the non-BSH hypertensive patients and 19% (n=6) of the BSH patients fulfilled criteria for indeterminate function (**Figure 3**).

Characteristics of LA size and function are presented in **Table 3**. Looking at 2D and 3D volume measurements, there were no significant group differences in LA size or in LA ejection fraction. However, the passive emptying fraction, related to LA conduit function, was significantly lower in the BSH subgroup resulting in significantly larger pre-atrial contraction volumes in these patients. Furthermore, BSH was associated with augmented LA contractile

function – higher active emptying volumes and higher contribution of active emptying to LV filling volume.

Left atrial deformation patterns of representative participants from each subgroup are shown in **Figure 4**. Both hypertensive patient groups had notably lower LA reservoir strain as compared to healthy controls. Conduit strain was significantly lower in hypertensive patients with BSH, while the contractile strain was higher. The change in LA dynamics was quantified with the subgroup differences in the LA conduit to contractile ratio. Phasic volumes calculated from 3D measurements correlated with corresponding strain measurements (see **Supplementary Materials**).

Discussion

BSH was present in 19.6% of our hypertensive cohort with well controlled hypertension. Patients with BSH were older, but with no differences in comorbidities or antihypertensive therapy as compared to non-BSH patients. BSH was related to decreased regional LV deformation, signs of impaired LV relaxation and a higher rate of indeterminate LV diastolic function. While LA size was similar, functional remodeling of the LA was seen in the BSH subgroup with a significant shift from an early to a late filling pattern - as demonstrated by the mitral inflow velocities, annular motion, LA phasic volumes and the LA conduit and contractile strain.

The echocardiographic finding of BSH has been shown to be predictive of arterial hypertension, suggesting that it may be a morphological marker of increased afterload.[1] Localized BSH and changes in deformation can be attributed to regional disparities in wall stress. Differences in local radius of curvature of the LV myocardial wall result in a heterogeneous wall stress distribution with a decrease from base to apex[10,11]. The septum is shown to have a greater

radius of curvature compared to the free wall[12,13]. In a normal blood pressure setting the right ventricle normalizes the transmural pressure across the septum, and thus compensates for the flatness of the region. With the rise in systemic blood pressure this compensation becomes insufficient, and the increase in wall stress becomes disproportionately higher in the basal parts of the septum[13], creating an imbalance between locally developed force and wall stress, and leading to decreased local deformation. With prolonged exposure to increased afterload, this imbalance may trigger cell mechanisms that result in the development of compensatory localized hypertrophy in an attempt to normalize wall stress and maintain deformation. In accordance with this, our results show the septum is thicker than the posterolateral wall in the hypertensive group, a finding also seen in magnetic resonance (MR) studies measuring wall thickness in hypertensive patients[14], but not in the MR studies of the healthy population[12]. Furthermore, we show a decrease of basal inferoseptal deformation, pronounced in the BSH patients, where it was combined with thickening of the basal septal wall - suggesting incomplete compensation of high wall stress in this subgroup.

At initial assessment, the only difference between the two hypertensive subgroups appeared to be BSH. With further analysis, we saw LV geometry classification signal a shift towards more advanced LV remodeling. There was further decrease of regional LV deformation related to BSH, and a typical pattern of impaired LV relaxation - determined by the IVRT, mitral and pulmonary vein inflow and mitral annular velocities[15]. This was coupled with a higher proportion of patients demonstrating indeterminate diastolic dysfunction – a classification previously associated with intermediate diastolic impairment[16]. LA assessment in BSH showed a reduction in LA reservoir function as compared to healthy controls, and a pronounced reduction in LA conduit together with an increase in LA contractile function compared to the non-BSH subgroup. LA functional compensatory mechanisms serve as acute regulators of LA performance

in response to impairment of LV filling[17,18], showing a decreased atrial conduit function coupled with a compensatory, augmented contractile function in early stages of LV filling impairment. The analysis of atrial function with 2D and 3D LA phasic-volume indices further confirmed these findings. Abnormalities in LA function have been previously shown in patients with hypertension without decreased LV global systolic performance and without LA enlargement[19–21]. Overall, our findings indicate further LA functional impairment in hypertensive patients with BSH, potentially increasing the cardiovascular risk of this subgroup [22].

This is a medium size single-center cohort of hypertensive patients with well-controlled blood pressure. Although our cohort is not representative of the whole hypertensive spectrum, the impairment associated to BSH was seen even in these well-controlled patients. We applied a previously used cut-off value for the basal-to-mid septal wall thickness ratio. Reassuringly, the prevalence of BSH and the reproducibility of septal measurements corresponded to data seen in previous publications[1,3,8]. The linear method of LV mass assessment is flawed in the presence of asymmetric hypertrophy. Additional exploration of this topic can be found in the **Supplementary Materials**. The age difference in our study should not result in any considerable differences in strain values, nevertheless, this could be a potential limitation. Localized hypertrophy of the basal region can also be seen in hypertrophic cardiomyopathy (HCM). Unfortunately, genetic information was not available in our cohort. However, family histories of disease or sudden cardiac death, as well as the patient's electrocardiograms were reviewed and none had positive findings. The heterogenic deformation pattern seen in HCM[23] was not noted in our cohort either. Moreover, the wall thickness seen in the BSH subgroup was lower than the criteria for HCM (basal inferoseptum median was 13 mm compared to the 15 mm cut-off in the guidelines[24]). Finally, echocardiographic data prior to the onset of hypertension or data on extended blood

pressure monitoring was not available. These data would be crucial to explore why selected patients with arterial hypertension develop BSH.

In conclusion, BSH is commonly seen in arterial hypertension. Changes in LV and LA function are already present in well-regulated patients with early LV remodeling and localized hypertrophy. Patients with BSH demonstrate decreased regional LV systolic deformation and impaired LV relaxation with a higher level of indeterminate diastolic dysfunction, coupled with more LA functional impairment, potentially increasing their cardiovascular risk. Therefore, the presence of BSH might be useful as a marker of the burden of hypertensive heart disease.

Acknowledgments

This work was supported by Horizon 2020 European Commission Project H2020-MSCA-ITN- 2016 (764738), Grant from Fundacio La Marató de TV3 (040310, Exp 2015.40.30), and from Fondo de Investigaciones Sanitarias - Instituto de Salud Carlos III (PI17/ 01131).

References

1. Gaudron PD, Liu D, Scholz F, Hu K, Florescu C, Herrmann S, Bijnens B, Ertl G, Störk S, Weidemann F. The septal bulge—an early echocardiographic sign in hypertensive heart disease. *J Am Soc Hypertens* 2016;10:70–80.

2. Baltabaeva A, Marciniak M, Bijnens B, Moggridge J, He F, Antonios T, Macgregor G, Sutherland G. Regional left ventricular deformation and geometry analysis provides insights in myocardial remodelling in mild to moderate hypertension. Eur J Echocardiogr 2007;4:501–508.

3. Verdecchia P, Porcellati C, Zampi I, Schillaci G, Gatteschi C, Battistelli M, Bartoccini C, Borgioni C, Ciucci A. Asymmetric left ventricular remodeling due to isolated septal thickening in patients with systemic hypertension and normal left ventricular masses. *Am J Cardiol* 1994;73:247–252.

4. Ranasinghe I, Ayoub C, Cheruvu C, Freedman SB, Yiannikas J. Isolated hypertrophy of the basal ventricular septum: Characteristics of patients with and without outflow tract obstruction. *Int J Cardiol* 2014;173:487–493.

5. Diaz T, Pencina MJ, Benjamin EJ, Aragam J, Fuller DL, Pencina KM, Levy D, Vasan RS. Prevalence, Clinical Correlates, and Prognosis of Discrete Upper Septal Thickening on Echocardiography: The Framingham Heart Study. *Echocardiography* 2009;26:247–253.

6. Chen-Tournoux A, Fifer MA, Picard MH, Hung J. Use of Tissue Doppler to Distinguish Discrete Upper Ventricular Septal Hypertrophy from Obstructive Hypertrophic Cardiomyopathy. *Am J Cardiol* 2008;101:1498–1503.

7. Yalçin F, Yiğit F, Erol T, Baltali M, Korkmaz ME, Müderrisoğlu H. Effect of dobutamine stress on basal septal tissue dynamics in hypertensive patients with basal septal hypertrophy. *J Hum Hypertens* 2006;20:628–630.

8. Lewis JF, Maron BJ. Diversity of patterns of hypertrophy in patients with systemic hypertension and marked left ventricular wall thickening. *Am J Cardiol* 1990;65:874–881.

9. Lang RM, Badano LP, Mor-Avi V, Afilalo J, Armstrong A, Ernande L, Flachskampf FA, Foster E, Goldstein SA, Kuznetsova T, Lancellotti P, Muraru D, Picard MH, Rietzschel ER, Rudski L, Spencer KT, Tsang W, Voigt J-U. Recommendations for Cardiac Chamber Quantification by Echocardiography in Adults: An Update from the American Society of Echocardiography and the European Association of Cardiovascular Imaging. *Eur Heart J – Cardiovasc Imaging* 2015;16:233–271.

10. Büchi M, Hess OH, Murakami T, Krayenbuehl HP. Left ventricular wall stress distribution in chronic pressure and volume overload: effect of normal and depressed contractility on regional stress-velocity relations. *Basic Res Cardiol* 1990;85:367–383.

11. Grossman W, Jones D, McLaurin LP. Wall stress and patterns of hypertrophy in the human left ventricle. *J Clin Invest* 1975;56:56–64.

12. Bogaert J, Rademakers FE. Regional nonuniformity of normal adult human left ventricle. *Am J Physiol-Heart Circ Physiol* 2001;280:H610–H620.

13. Heng MK, Janz RF, Jobin J. Estimation of regional stress in the left ventricular septum and free wall: An echocardiographic study suggesting a mechanism for asymmetric septal hypertrophy. *Am Heart J* 1985;110:84–90.

14. Goh VJ, Le T-T, Bryant J, Wong JI, Su B, Lee C-H, Pua CJ, Sim CPY, Ang B, Aw TC, Cook SA, Chin CWL. Novel index of maladaptive myocardial remodeling in hypertension. Circ Cardiovasc Imaging 2017;10:e006840.

15. Zile MR, Brutsaert DL. New Concepts in Diastolic Dysfunction and Diastolic Heart Failure: Part I: Diagnosis, Prognosis, and Measurements of Diastolic Function. *Circulation* 2002;105:1387–1393.

16. Sanchis L, Andrea R, Falces C, Poyatos S, Vidal B, Sitges M. Differential Clinical Implications of Current Recommendations for the Evaluation of Left Ventricular Diastolic Function by Echocardiography. *J Am Soc Echocardiogr* 2018;31:1203–1208.

17. Kono T. Left atrial contribution to ventricular filling during the course of evolving heart failure. *Circulation* 1992:1317–1322.

18. Prioli A, Marino P, Lanzoni L, Zardini P. Increasing degrees of left ventricular filling impairment modulate left atrial function in humans. *Am J Cardiol* 1998;82:756–761.

19. Fouad FM, Slominski JM, Tarazi RC. Left ventricular diastolic function in hypertension: relation to left ventricular mass and systolic function. *J Am Coll Cardiol* 1984;3:1500–1506.

20. Mondillo S, Cameli M, Caputo ML, Lisi M, Palmerini E, Padeletti M, Ballo P. Early Detection of Left Atrial Strain Abnormalities by Speckle-Tracking in Hypertensive and Diabetic Patients with Normal Left Atrial Size. *J Am Soc Echocardiogr* 2011;24:898–908.

21. Liu Y, Wang K, Su D, Cong T, Cheng Y, Zhang Y, Wu J, Sun Y, Shang Z, Liu J, Zhong L, Zou L, Chitian C, Zhang X, Jiang Y. Noninvasive Assessment of Left Atrial Phasic Function in

Patients with Hypertension and Diabetes Using Two-Dimensional Speckle Tracking and Volumetric Parameters. *Echocardiography* 2014;31:727–735.

22. Modin D, Biering-Sørensen SR, Møgelvang R, Alhakak AS, Jensen JS, Biering-Sørensen T. Prognostic value of left atrial strain in predicting cardiovascular morbidity and mortality in the general population. *Eur Heart J - Cardiovasc Imaging* 2019;20:804–815.

23. Cikes M, Sutherland GR, Anderson LJ, Bijnens BH. The role of echocardiographic deformation imaging in hypertrophic myopathies. *Nat Rev Cardiol* 2010;7:384–396.

24. The Task Force for the Diagnosis and Management of Hypertrophic Cardiomyopathy of the European Society of Cardiology (ESC). 2014 ESC Guidelines on diagnosis and management of hypertrophic cardiomyopathy: the Task Force for the Diagnosis and Management of Hypertrophic Cardiomyopathy of the European Society of Cardiology (ESC). Eur Heart J 2014;35:2733–2779.

Tables

Table 1. Clinical characteristics of the cohort

Variable	Healthy controls (n=22)	Basal septal hypertrophy		Group P value
		No (n=131)	Yes (n=32)	
Age (*years)*	54 (51-54)	57 (53-60)	60 (55-63)*†	**0.001**
Men	10 (46%)	68 (52%)	21 (66%)	0.280
Body mass index (*kg/m2)*	24.8±2.7	28.0±4.5*	28.8±3.6*	**0.001**
Body surface area (m^2)	1.93±0.18	1.91±0.23	1.99±0.20	0.189
Duration of hypertension (*years)*	-	8 (5-14)	9 (6-15)	0.274
Systolic blood pressure (*mmHg)*	124±12	136±16*	142±15*	**<0.001**
Diastolic blood pressure (*mmHg)*	81±8	79±10	82±10	0.279
Heart rate (*beats per minute)*	62±8	67±10*	69±10*	**0.020**
Diabetes mellitus	0	14 (11%)*	6 (19%)*	0.081
Dyslipidemia	0	66 (51%)	18 (56%)	0.694
Treated with two or more antihypertensive drugs	0	64 (49%)	22 (69%)	0.050

Treated with three or more drugs	0	18 (14%)	6 (19%)	0.577
Beta blocker	0	27 (21%)	7 (22%)	1
Aldosterone receptor blockers	0	54 (41%)	15 (47%)	0.690
Angiotensin-converting enzyme inhibitor	0	50 (38%)	15 (47%)	0.422
Calcium antagonists	0	35 (27%)	9 (28%)	1
Angiotensin-converting enzyme inhibitor or calcium antagonists	0	74 (57%)	21 (66%)	0.425
Diuretics	0	44 (34%)	13 (41%)	0.536
Statins	0	26 (20%)	10 (31%)	0.233
Any lipid lowering drug	0	40 (31%)	11 (34%)	0.674
** P<0.05 versus healthy controls* *† P<0.05 versus patients without basal septal hypertrophy*				

1
2

Table 2. Characteristics of LV size and function

Variables	Healthy controls (n=22)	Basal septal hypertrophy		Group P value
		No (n=131)	Yes (n=32)	
LV ejection fraction *(%)*	58 (54-60)	55 (53-58)	61 (56-64)†	**<0.001**
LV global longitudinal strain *(%)*	-20.92±2.78	-21.14±2.37	-20.28±3.14	0.238
LV end-systolic volume *(ml)*	45 (38-52)	47 (41-59)	36 (30-43)†	**<0.001**
LV end-diastolic volume *(ml)*	103 (92-115)	107 (94-129)	92 (80-113)†	**0.003**
Posterior wall thickness *(mm)*	0.8 (0.8-1.0)	1.1 (1.0-1.2)*	1.1 (1.0-1.2)*	**<0.001**
Basal-to-mid anteroseptal wall thickness ratio	1.1 (1.0-1.2)	1.1 (1.0-1.2)	1.4 (1.2-1.6)*†	**<0.001**
Basal-to-mid inferoseptal wall thickness ratio	1.1 (1.0-1.2)	1.1 (1.0-1.3)	1.6 (1.4-1.7)*†	**<0.001**
Indexed LV mass *(g/m2)*	66.5 (53.8-78.7)	75.6 (66.1-89.0)*	93.3 (81.3-101.5)*†	**<0.001**
Relative wall thickness	0.37 (0.34-0.39)	0.52 (0.44-0.59)*	0.55 (0.48-0.60)*	**<0.001**
Normal LV geometry	18 (82%)	22 (17%)	0	**<0.001**
Concentric remodeling	4 (18%)	100 (77%)	28 (88%)	
Concentric hypertrophy	0	8 (6%)	4 (12%)	

Isovolumic relaxation time (*ms)*	80 (74-90)	85 (79-95)	90 (79-97)	0.055
E velocity (*cm/s)*	75±14	72±14	66±19	0.063
E deceleration time (*ms)*	191±36	194±37	195±39	0.718
A velocity (*cm/s)*	64±15	72±14*	78±13*	**0.006**
A duration (*ms)*	115 (107-127)	125 (115-135)*	130 (118-145)*	**0.006**
E/A ratio	1.17 (0.97-1.36)	0.99 (0.82-1.17)*	0.82 (0.70-1.01)*†	**<0.001**
Pulmonary vein S velocity (*cm/s)*	59±8	58±9	55±8	0.207
Pulmonary vein D velocity (*cm/s)*	44 (41-48)	41 (37-47)	38 (34-42)*	**0.019**
Pulmonary vein S/D ratio	1.37±0.21	1.40±0.26	1.46±0.28	0.454
Pulmonary vein A velocity (*cm/s)*	31 (29-34)	27 (25-29)*	27 (24-29)*	**<0.001**
Mitral annulus septal e' velocity (*cm/s)*	8.0 (7.0-9.0)	8.0 (7.0-10.0)	7.0 (6.0-8.0)*†	**<0.001**
Mitral annulus lateral e' velocity (*cm/s)*	-	11.0 (9.0-13.0)	9.0 (8.0-11.0)	**0.012**
Mitral annulus septal a' velocity (*cm/s)*	10.0 (9.0-11.3)	10.0 (8.0-11.0)	11.0 (9.0-12.0)†	**0.032**
Mitral annulus lateral a' velocity (*cm/s)*	-	10.0 (9.0-13.0)	12.0 (9.3-13.0)	0.221
Tricuspid annular plane systolic excursion (*mm)*	27±3	23±4*	21±4*†	**<0.001**

** P<0.05 versus healthy controls*
† P<0.05 versus patients without basal septal hypertrophy

Table 3. Characteristics of LA size and function

Variables		Healthy controls (n=22)	Basal septal hypertrophy		P value
			No (n=131)	Yes (n=32)	
LA maximal volume (*ml/m²)*	2D	28.5 (21.2-32.4)	27.8 (24.0-31.9)	31.1 (26.3-34.2)	0.152
	3D	-	31.9 (25.5-37.2)	32.2 (27.4-38.4)	0.226
LA minimal volume, (*ml/m²)*	2D	10.4 (9.2-16.1)	12.5 (10.3-15.8)	14.3 (12.1-17.4)	0.084
	3D	-	13.5 (11.4-16.4)	16.5 (11.4-18.3)	0.069
LA pre-atrial contraction volume, (*ml/m²)*	2D	19.1(15.8-25.0)	20.1 (17.4-24.0)	23.2 (20.2-27.6)†	**0.019**
	3D	-	20.7 (17.0-24.6)	22.9 (20.4-22.9)	**0.011**
LA ejection fraction (%)	2D	55±9	54± 8	52±7	0.678
	3D	-	55±7	54±6	0.605
LA stroke volume, (*ml/m²)*	2D	14.9 (11.7-16.9)	15.2 (12.4-17.4)	15.6 (12.9-18.6)	0.558
	3D	-	16.9 (14.0-20.9)	16.8 (15.5-20.4)	0.646
LA passive emptying fraction *(%)*	2D	28±9	27±8	22±9*†	**0.015**
	3D	-	32±9	27±9†	**0.005**

LA passive emptying volume, (*ml/m²)*	2D	7.0 (5.1-9.1)	7.4 (6.0-9.2)	8.3 (7.2-10.6)	0.056
	3D	-	6.7 (5.4-8.6)	8.2 (6.5-11.3)†	**0.005**
LA active emptying fraction (*%*)	2D	37±9	37±13	38±9	0.761
	3D	-	33±9	37±8	0.066
LA active emptying volume (*ml/m²)*	2D	7.0 (5.1-9.1)	7.5 (5.9-9.2)	8.3 (7.2-10.6)	0.059
	3D	-	6.7 (5.4-8.8)	8.2 (6.5-10.7)†	**0.005**
LA active contribution to LV filling (%)	2D	50±13	50±16	57±16*†	**0.040**
	3D	-	40 (32-49)	50 (40-60)†	**0.003**
LA reservoir strain *(%)*	2D	32.37±4.04	29.59±4.89*	28.48±4.67*	**0.020**
LA conduit strain *(%)*	2D	18.78±3.67	14.59±3.75*	11.78±3.60*†	**<0.001**
LA contractile strain (%)	2D	13.58±2.42	14.99±2.81	16.70±4.02*†	**<0.001**
LA conduit to contractile ratio	2D	1.50 (1.16-1.73)	0.95 (0.78-1.17)*	0.71 (0.50-0.94)*†	**<0.001**

** P<0.05 versus healthy controls*
† P<0.05 versus patients without basal septal hypertrophy

Figure legends

Figure 1. Images demonstrating measurement of basal septal and mid-septal wall thickness in parasternal long-axis (*left*) and 4-chamber (*right*) views.

Figure 2. Comparison of the antero- and inferoseptal wall thickness measured in PLAX and 4-chamber views, respectively; and regional LV deformation between subgroups, as assessed by speckle-tracking in the 4-chamber view. A trend in basal and mid-segmental impairment can be seen in the hypertensive subgroups (*dotted arrows*), significantly pronounced in patients with BSH (*full arrow)*. *(*P<0.05 versus healthy controls, †P<0.05 versus patients without BSH)*

Figure 3. Diastolic dysfunction assessment as proposed by current recommendations shows higher incidence of indeterminate diastolic dysfunction in hypertensive patients with BSH.

Figure 4. Comparison of LV morphology (*top images*) and LA function (*bottom images*) between healthy controls (*left*), hypertensive patients without BSH (*middle*), and hypertensive patients with BSH (*right*). The scale of shown strain curves is equal in all patients. A reduction in LA reservoir strain can be seen in the hypertensive patients, coupled with an increase in LA contractile and reduction of LA conduit function.

Figure legends

Figure 1

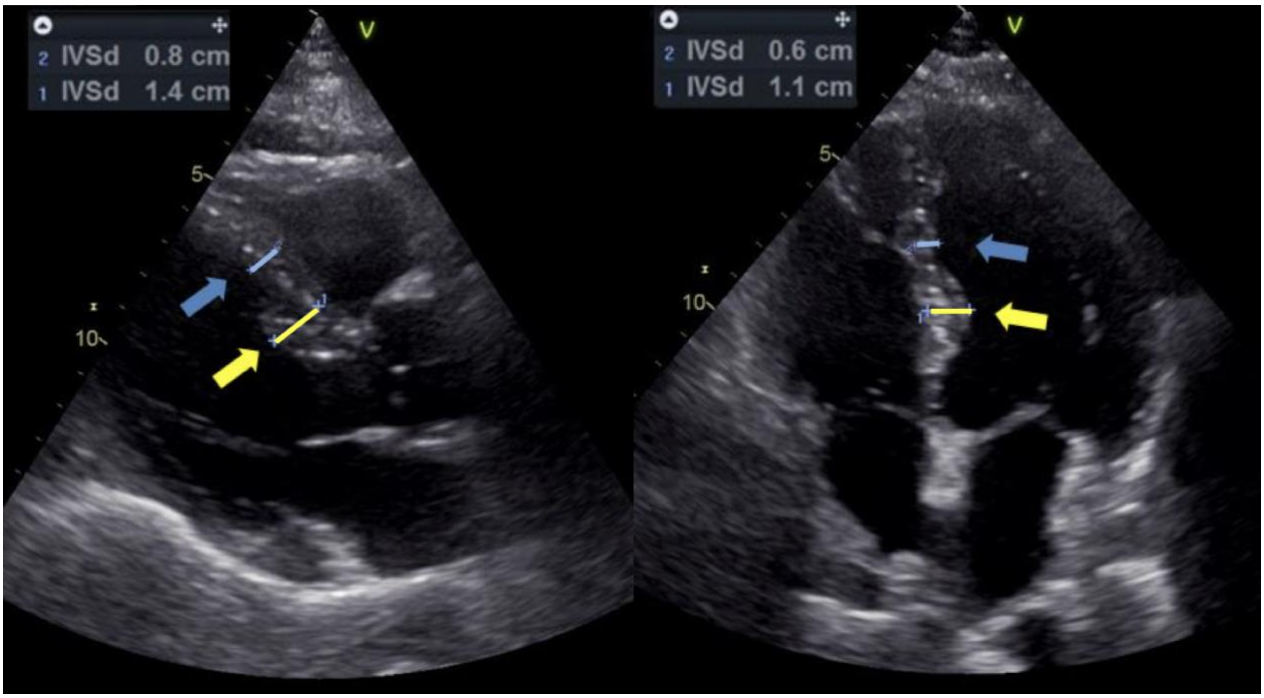

Figure 2

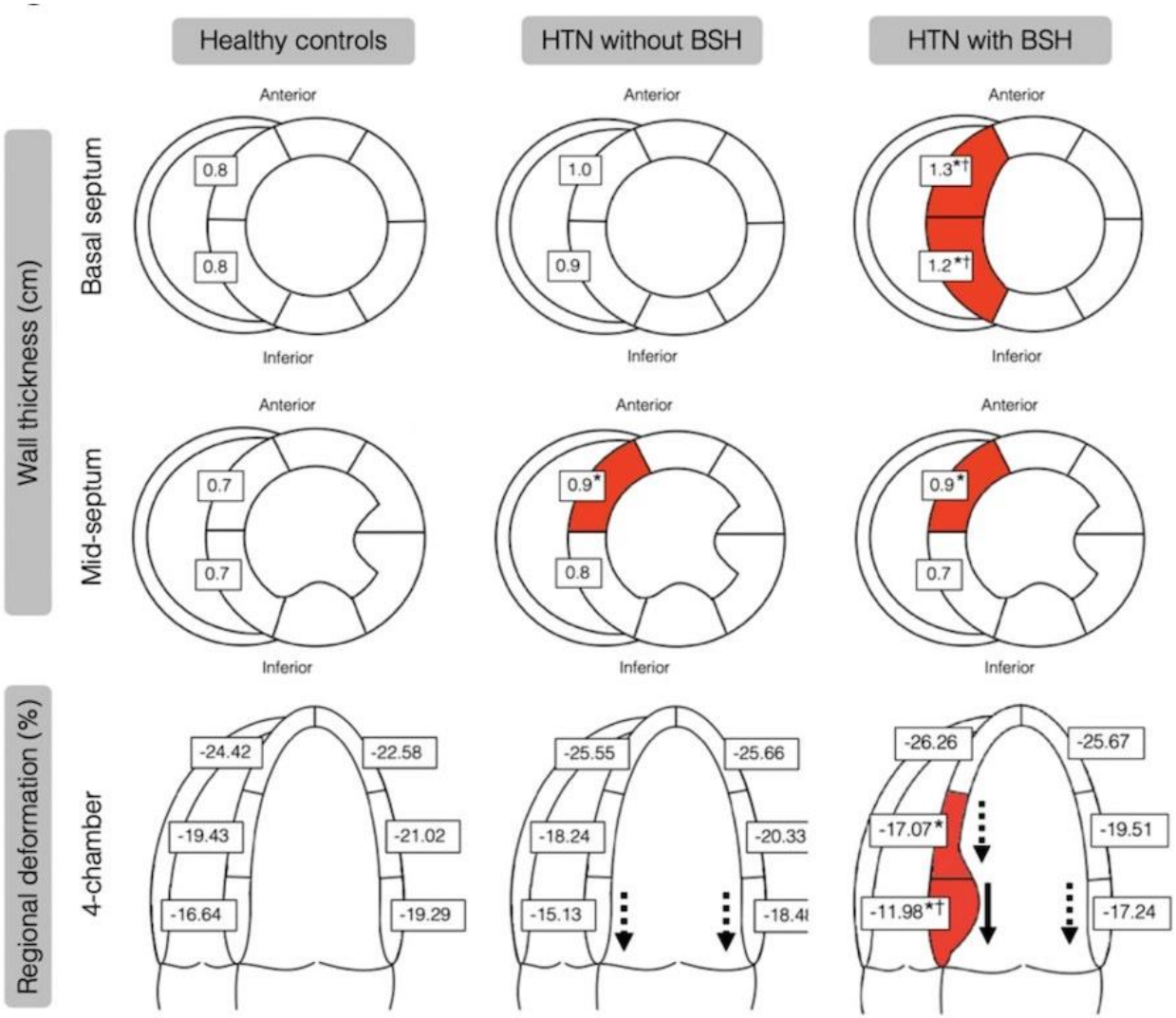
Healthy controls
HTN without BSH
HTN with BSH
Wall thickness (cm)
Basal septum
Mid-septum
Regional deformation (%)
4-chamber
Anterior
Inferior
0.8
0.8
1.0
0.9
1.3*†
1.2*†
0.7
0.7
0.9*
0.8
0.9*
0.7
-24.42
-22.58
-19.43
-21.02
-16.64
-19.29
-25.55
-25.66
-18.24
-20.33
-15.13
-26.26
-25.67
-17.07*
-19.51
-11.98*†
-17.24

Figure 3

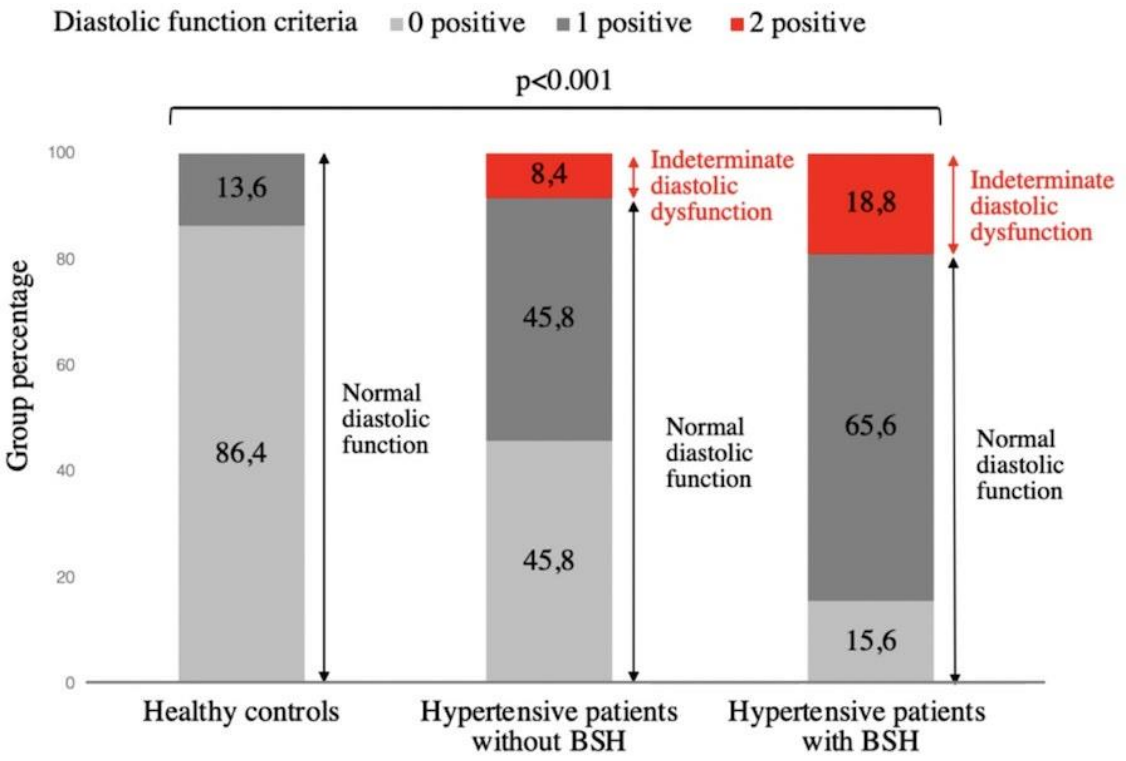

Figure 4

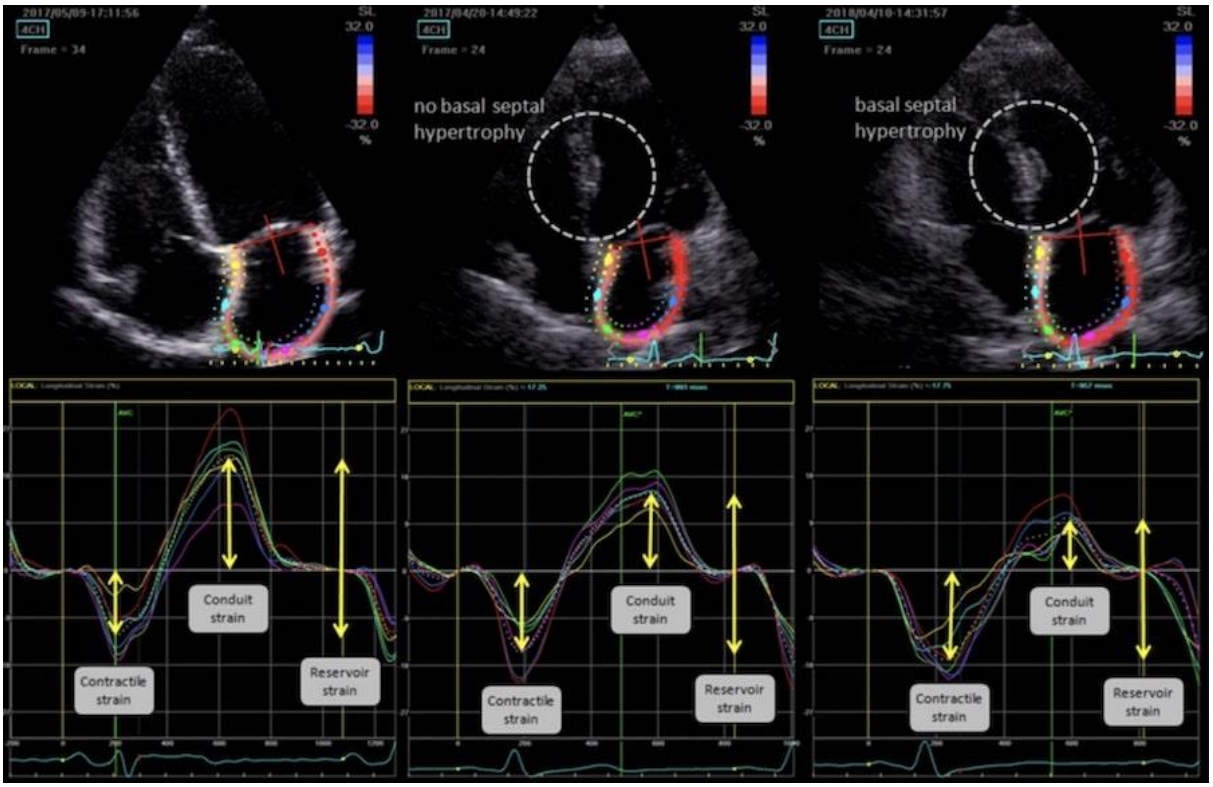

Supplementary Materials
Expanded Methods

Echocardiography

LV and LA volumes were assessed in the apical 4- and 2-chamber views. LV ejection fraction was calculated by using the biplane Simpson method. Pulsed-wave Doppler was performed in the apical 4-chamber view by placing the sample volume at the level of the leaflet tips to obtain mitral inflow velocities. Peak velocity of early (E) and late (A) diastolic filling, E velocity deceleration time and A wave duration were measured, and the E/A ratio calculated. Isovolumic relaxation time (IVRT) was measured as the time difference between aortic valve closure and mitral valve opening as assessed in the five-chamber view using continuous-wave Doppler of the LV outflow tract. Pulmonary vein inflow was recorded in the 4-chamber view with pulsed-wave Doppler and the peak early systolic (S), early diastolic (D) and late diastolic (A) velocities were recorded and the S/D ratio calculated. Tissue Doppler was used to measure early and late diastolic mitral annular velocity at the septal (e' and a' septal) and lateral (e' and a' lateral) annular sites. Diastolic function was assessed according to the current recommendations and classified as normal function, indeterminate function, or developed diastolic dysfunction[1].

Regional myocardial deformation of the LV was assessed using speckle tracking echocardiography software on 2D grayscale images obtained from the apical 4-chamber view. The endocardial border was manually marked at end-systole of the LV. A region of interest with six segments was automatically generated. If needed, manual adjustments were performed to achieve optimal tracking. Segments without adequate tracking were excluded from the analysis, whereas patients with inadequate tracking of more than 3 segments were excluded from the study. Longitudinal strain curves were generated and end-systolic strain, defined by the aortic

valve closure time, was measured. LV global longitudinal strain (LVGLS) was calculated by averaging values of the segments.

The analysis of LA deformation was performed similarly to the process described for the LV, in the 4- and 2-chamber apical views. Longitudinal strain curves were generated. Using the P wave as the onset for deformation analysis, left atrial reservoir, conduit, and contractile function were evaluated by measuring LA systolic, early diastolic and late diastolic strain, respectively and averaged from the 4- and 2-chamber measurements.

LA function was assessed by phasic changes in LA volumes and by myocardial deformation. Using 2D and 3D measurements, respectively, phasic LA volumes were assessed to capture the minimal, maximal, and the volume before atrial contraction at the beginning of the P wave. Standard indexes of LA function were calculated using volumes indexed to the BSA. Total ejection fraction was calculated as the difference of maximal and minimal volume divided by maximal volume. Active emptying fraction was calculated as the difference of the volume at the beginning of the P wave and minimal volume divided by the volume at the beginning of the P wave. Finally, passive emptying fraction was calculated as the difference of the maximal volume and the volume at the beginning of the P wave divided by the maximal volume. The active contribution to LV filling was calculated as [(volume at the beginning of the P wave–minimal volume)/(maximal volume–minimal volume)]×100.

Calculation of LV mass and relative wall thickness

Current guidelines [2] recognize that the commonly used M-mode or 2D echocardiography based methods of assessing LV mass are inaccurate in the setting of asymmetric hypertrophy. In the setting of BSH, the linear method of LV mass assessment, using the Cube formula ($LV\ mass = 0.8 \times 1.04 \times [(IVS + LVID + LVPWd)^3 - LVID^3] + 0.6g$) results in

overestimation of the true mass due to the incorporation of the thick localized hypertrophy in the region of the basal septum (in the formula: interventricular septum - IVS). On the other hand, the area-length method, which uses mid-ventricular measurements instead of basal measurements, will underestimate LV mass, due to the fact that the region of hypertrophy is not included in the measurement. For asymmetric hearts, 3D echocardiography is the only echocardiography-based method that is non-dependent on geometric assumptions, and which has been previously shown to be reliable in assessing asymmetric hypertrophy in hypertrophic cardiomyopathy[3]. Considering the lack of 3D LV data on LV mass in our cohort, we used the linear method to calculate the LV mass using both mid-septal and basal septal wall thickness for the IVS variable, respectively. LV mass was then normalized by body surface area (BSA), and sex-dependent cut-off values were used to indicate LV hypertrophy. Relative wall thickness (RWT) was calculated by dividing the doubled value of the end-diastolic posterior wall thickness with the end-diastolic internal diameter of the LV. The type of LV remodeling was determined based on the RWT and indexed LV mass. Patients with normal LV mass were categorized as having normal geometry or concentric remodeling, while the patients with increased LV mass as concentric or eccentric hypertrophy[2].

Intra-observer and inter-observer reproducibility of measurements

Reproducibility of results was assessed for LV GLS, LA contractile strain, LA conduit strain, and the basal septal wall thickness measurements in both the 4-chamber and PLAX views. With a two-month interval between measurements, 15 randomly selected patients were remeasured by the first investigator blinded to the original results. The same patients were then measured by a second investigator, also blinded to the original results. Analysis of bias and the calculation of 95% limits of agreement for intra- and inter-observer variability were performed

using the Bland-Altman method.[4] The coefficient of variation was also calculated to assess the variability of measurements.

Expanded Results

LA size and function

The dynamic relationship between LA deformation and LV relaxation was illustrated through the correlation of the LA conduit to contractile ratio with the E/A ratio (Pearson R 0.524, $p<0.001$) and the mitral annulus lateral e' velocity (Pearson R 0.437, $p<0.001$).

Phasic volumes calculated from 3D measurements correlated with corresponding strain measurements - LA reservoir strain with LA ejection fraction (Pearson R 0.446, $p<0.001$), LA conduit strain with LA passive emptying fraction (Pearson R 0.438, $p<0.001$), and LA contractile strain with LA active emptying fraction (Pearson R 0.386, $p<0.001$).

LV mass calculation

Results are shown in **Supplementary Table 1.** To explore the impact of BSH on the calculation of LV mass using the linear method, we used both the mid-septal and basal wall thickness in the cube equation, respectively. Using the mid-septal wall thickness undermines localized hypertrophy of the basal segment and hence underestimates true LV mass, resulting with the BSH patients having similar LV mass as in the non-BSH subgroup. When using basal wall thickness, the LV mass is overestimated and therefore significantly higher in the BSH subgroup compared to the non-BSH and healthy controls. It is sensible to conclude that the true LV mass of the BSH cohort is a value in between these two approximations. The corresponding categorizations of individuals into LV geometry groups will also be affected by these different approaches. When using mid-septal wall thickness in the calculations all patients with BSH were

categorized as having LV concentric remodeling, while the geometry was normal in up to 16% of hypertensives without BSH and in the majority of controls. As expected, when using basal septal wall thickness for the calculations, the categorization of healthy controls and non-BSH patients did not change significantly, while 12% of BSH patients were re-categorized into LV concentric hypertrophy. In conclusion, this data suggests that the true LV remodeling of BSH patients is somewhere in between the two categorization approaches – nevertheless implying that LV remodeling is further developed in patients with BSH then in those without.

Reproducibility of the results

Reproducibility of the results is shown in **Supplementary Figure 1** and **2**, **Supplementary Table 2**. Inter- and intraobserver variability of measuring LA contractile strain were 0.3% (95% CI: -6.1-6.7) and 0.7% (95% CI: -1.39-2.85); and of LA conduit strain 0.9% (95% CI: -3.9-5.8) and 0.9% (95% CI: -3.7-5.6), respectively. Inter- and intraobserver variability of basal septal measurements in 4-chamber was 0.06 cm (95% CI: -0.26-0.14) and 0.03 cm (95% CI: -0.20-0.15), while in the PLAX view 0.03 cm (95% CI: -0.14-0.21) and 0.03 cm (95% CI: -0.18-0.11), respectively. The coefficients of variability showed similarly low variation in all parameters.

Supplementary references

1 Nagueh SF, Smiseth OA, Appleton CP, Byrd BF, Dokainish H, Edvardsen T, Flachskampf FA, Gillebert TC, Klein AL, Lancellotti P, Marino P, Oh JK, Popescu BA, Waggoner AD. Recommendations for the Evaluation of Left Ventricular Diastolic Function by Echocardiography: An Update from the American Society of Echocardiography and the European Association of Cardiovascular Imaging. *J Am Soc Echocardiogr* 2016; **29**: 277–314.

2 Lang RM, Badano LP, Mor-Avi V, Afilalo J, Armstrong A, Ernande L, Flachskampf FA, Foster E, Goldstein SA, Kuznetsova T, Lancellotti P, Muraru D, Picard MH, Rietzschel ER, Rudski L, Spencer KT, Tsang W, Voigt J-U. Recommendations for Cardiac Chamber Quantification by Echocardiography in Adults: An Update from the American Society of Echocardiography and the European Association of Cardiovascular Imaging. *Eur Heart J – Cardiovasc Imaging* 2015; **16**: 233–271.

3 Chang S-A, Kim H-K, Lee S-C, Kim E-Y, Hahm S-H, Kwon OM, Park SW, Choe YH, Oh JK. Assessment of Left Ventricular Mass in Hypertrophic Cardiomyopathy by Real-Time Three-Dimensional Echocardiography Using Single-Beat Capture Image. *J Am Soc Echocardiogr* 2013; **26**: 436–442.

4 J Martin Bland, Douglas G Altman. Statistical methods for assessing agreement between two methods of clnical measurement. *The Lancet* 1986; : 307–310.

Supplementary Tables

Supplementary Table 1 Assessment of LV mass and RWT using the linear method

	Variable	Healthy controls (n=22)	Basal septal hypertrophy		Group P value
			No (n=131)	Yes (n=32)	
-	Indexed LV mass (*using basal septal wall thickness*) (*g/m2)*	66.5 (53.8-78.7)	75.3 (66.5-89.0)*	93.6 (81.2-100.6)*†	**<0.001**
-	Indexed LV mass (*using mid septal wall thickness*) (*g/m2)*	63.0 (53.3-73.3)	70.9 (62.1-83.9)*	70.0 (61.6-77.2)	**0.048**
-	Relative wall thickness	0.37 (0.34-0.39)	0.52 (0.44-0.59)*	0.55 (0.48-0.60)*	**<0.001**
Mid-septal wall thickness in calculation	Normal LV geometry	18 (82%)	22 (17%)	0	**<0.001**
Mid-septal wall thickness in calculation	Concentric remodeling	4 (18%)	102 (79%)	32 (100%)	
Mid-septal wall thickness in calculation	Concentric hypertrophy	0	6 (5%)	0	
Basal-septal wall thickness in calculation	Normal LV geometry	18 (82%)	22 (17%)	0	**<0.001**
Basal-septal wall thickness in calculation	Concentric remodeling	4 (18%)	100 (77%)	28 (88%)	
Basal-septal wall thickness in calculation	Concentric hypertrophy	0	8 (6%)	4 (12%)	

** P<0.05 versus healthy controls*
† P<0.05 versus patients without BSH

Supplementary Table 2 Analysis of bias and the calculation of 95% limits of agreement for interobserver and intraobserver variability in strain and wall thickness parameters.

Measurement		Intraobserver variability				Interobserver variability			
			95% Confidence Interval				95% Confidence Interval		
	N	Mean difference	Lower limit	Upper limit	CoV	Mean difference	Lower limit	Upper limit	CoV
Basal inferoseptum (cm)	15	-0,03	-0,20	0,15	0,04	-0,06	-0,26	0,14	0,06
Basal anteroseptum (cm)	15	-0,03	-0,18	0,11	0,04	0,03	-0,14	0,21	0,05
Mid-inferoseptum (cm)	15	-0,02	-0,15	0,11	0,04	-0,04	-0,32	0,24	0,10
Mid-anteroseptum (cm)	15	0,01	-0,22	0,23	0,07	-0,05	-0,42	0,32	0,11
Basal to mid-septum inferoseptal ratio	15	-0,01	-0,24	0,23	0,04	-0,01	-0,39	0,36	0,07
Basal to mid-anteroseptal ratio	15	0,03	-0,32	0,38	0,08	-0,01	-0,42	0,40	0,09
LV global longitudinal strain (%)	15	0,6	-5,6	4,4	0,06	0,8	-5,3	3,6	0,06
LA contractile strain (%)	15	0,7	-1,39	2,85	0,09	0.3	-6,1	6,7	0,07
LA conduit strain (%)	15	0,9	-3,7	5,6	0,14	0,9	-3,9	5,8	0,13

CoV – Coefficient of variation; 4C – 4-chambre view; PLAX – parasternal long axis view; LV – left ventricle, LA – left atrium

Supplementary Figure Legends

Supplementary Figure 1 Analysis of bias and the calculation of 95% limits of agreement for interobserver (*left*) and intraobserver (*right*) variability. Top row shows the Bland-Altman plots for variability in 4-chamber (4C) view measurements of LV global longitudinal strain; middle row shows variability in 4C view measurements for LA contractile strain; while the bottom row for 4C LA conduit strain.

Supplementary Figure 2 Analysis of bias and the calculation of 95% limits of agreement for interobserver (*left*) and intraobserver (*right*) variability. First and second row show the Bland-Altman plots for variability in 4-chamber (4C) and parasternal long-axis (PLAX) view measurements of basal septal wall thickness, respectively; the third and fourth row show variability in 4C and PLAX basal-to-mid septal wall thickness ratio, respectively.

Supplementary Figure Legends

Supplementary Figure 1

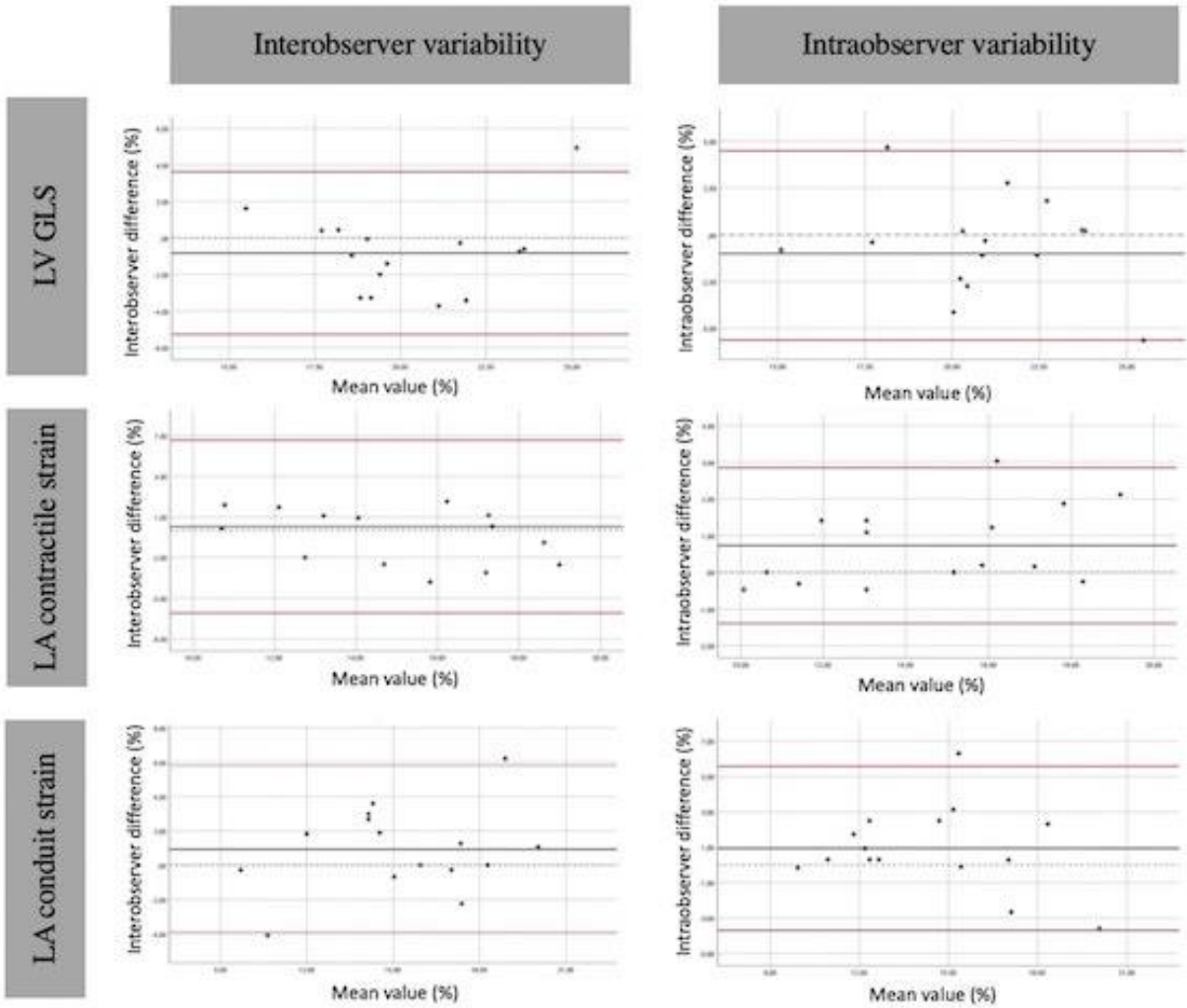

Supplementary Figure 2